Automatic Optic Disc Boundary Extraction from Color Fundus Images

Thresiamma Devasia

Dept. of Computer Science
Assumption College
Changanacherry, India

Paulose Jacob

Dept. of Computer Science
Cochin University of
Science and Technology
Cochin, India

Tessamma Thomas

Dept. of Electronics
Cochin University of
Science and Technology
Cochin, India

Abstract—**Efficient optic disc segmentation is an important task in automated retinal screening. For the same reason optic disc detection is fundamental for medical references and is important for the retinal image analysis application. The most difficult problem of optic disc extraction is to locate the region of interest. Moreover it is a time consuming task. This paper tries to overcome this barrier by presenting an automated method for optic disc boundary extraction using Fuzzy C Means combined with thresholding. The discs determined by the new method agree relatively well with those determined by the experts. The present method has been validated on a data set of 110 colour fundus images from DRION database, and has obtained promising results. The performance of the system is evaluated using the difference in horizontal and vertical diameters of the obtained disc boundary and that of the ground truth obtained from two expert ophthalmologists. For the 25 test images selected from the 110 colour fundus images, the Pearson correlation of the ground truth diameters with the detected diameters by the new method are 0.946 and 0.958 and, 0.94 and 0.974 respectively. From the scatter plot, it is shown that the ground truth and detected diameters have a high positive correlation. This computerized analysis of optic disc is very useful for the diagnosis of retinal diseases.**

Keywords—fundus image; optic nerve head; optic disc; Fuzzy C-Means clustering

I. INTRODUCTION

The fundus images are used for diagnosis by trained clinicians to check any abnormality or any sort of change in the retina. A healthy retinal image contains anatomical structures like the macula, the optic disc and blood vessels. The retinal optic disc is the region from where the optic nerve of the retina emanates. Hence, it often serves as an important landmark and reference for other features in a retinal fundus image. The optic disc (OD) in a healthy retinal image usually appears as a bright yellowish and circular shaped object which is partly covered with blood vessels. Diseases with symptoms on the fundus images are very complex. For the OD, differences in the color, shape, edge or vasculature may signify a pathological change [1]. The information about the OD can be used to detect the severity of some diseases such as glaucoma.

An efficient segmentation of the OD is essential to diagnose various stages of many retinal diseases. The optic disc appears as an elliptical region with high intensity in retinal images [2]. The method of optic disk boundary detection can be separated into two steps: optic disc extraction and disc boundary detection.

Many existing techniques can be used with reasonable success to extract the optic disc and disc boundary. Huiqi Li et al. [3] designed yet another method based on Principle Component Analysis to localize OD automatically. Snake Active Contour methodology for optical disc detection was proposed by Thitiporn et al. [4]. The contrast of the optical disc is used as the significant feature in this work. But the initialization of size and shape of the contour is in fact, a practical difficulty of this approach.

A novel method to locate the optic nerve in fundus images was developed by Hoover A. et al. [5]. They used Fuzzy convergence to determine the origin of the blood vessel network. Hough Transform was used for OD detection by Chrastek et al. [6]. Juan Xu et al. [7] used a modified Active Contour Model for OD detection. The smoothing update equation of Snake model is modified and used in this approach for performance enhancement. Genetic Algorithm (GA) based optic disk detection is reported by Enrique et al.[8]. Echegaray et al.[9] developed a method for automatic initialization of a level-set segmentation algorithm to find the margin of the optic disc in fundus images as an indicator for glaucoma.

A method to automatically segment the optic using morphological approach was developed by Welfer D et al.[10] Siddalingaswamy et al. [11] proposed a method for automatic localization and accurate boundary detection of OD using iterative thresholding technique. Yuji Hatanaka, et al. [12] used a Canny edge detection filter for OD edge detection. Amin Dehghani et al. [13] designed histogram matching technique for OD localization. Angel Suero et al.[14] used morphological techniques for OD localization. Fuzzy C Means Clustering with thresholding is used in this work for the extraction of optic disc. Fuzzy C-Means is an unsupervised technique that has been successfully applied for feature analysis, clustering, and to classify designs in the fields such as geology, medical imaging and image segmentation.

The rest of the paper is organized as follows. Section II describes the materials used for the new method. In Section III, a new algorithm for the efficient extraction of optic disc boundary ocular fundus images is presented. The results are presented in Section IV, and conclusions are given in Section V.

II. MATERIALS AND METHODS

All the images used in this paper are obtained from the DRION database. There are 110 retinal colour fundus images

with an array size of $400 \times 600 \times 3$ pixels, along with the optic nerve contours traced by two experts.

III. ALGORITHM DEVELOPED

The algorithm is composed mainly of four steps. First, the red channel of the colour retinal image is separated. Then the blood vessels are removed. Thirdly the Fuzzy C Means Clustering operation is applied on the vessel-free image. Thresholding is used for the extraction of OD from this image. The boundary of the extracted OD is traced and, finally this extracted boundary is overlaid on the ground truth image. Performance analysis is done comparing the detected diameters with the ground truth diameters. Statistical analysis is done using scatter plot, which gives high positive correlation between the detected boundary and ground truth boundary.
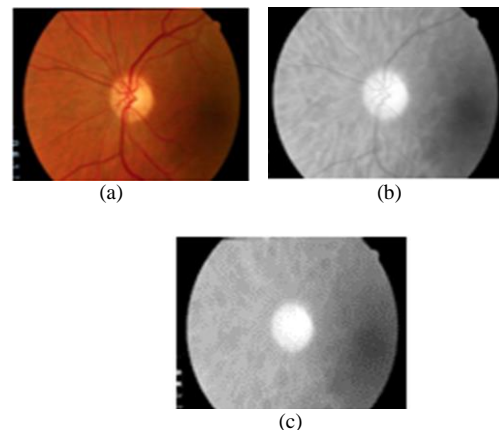
A. Preprocessing

The preprocessing step removes variations due to image acquisition, such as inhomogeneous illumination [15]. Techniques such as morphological operations are applied to the input image. The following sessions elaborate the different preprocessing operations used in this paper.

1) Selection of Red Channel
In fundus images, the optic disc belongs to the brightest point of the image. The OD is often present in the red field as a well-defined white shape, brighter than the surrounding area. This color channel provides the highest contrast between OD and back ground [16]. So the red channel of the RGB colour image is used in this paper for the extraction of optic disc regions in the retinal fundus images.

2) Removal of blood vessels
Blood vessels within the OD act as strong distracters, and so they should be erased from the image beforehand. Mathematical morphology can extract important shape characteristics and also remove irrelevant information. It typically probes an image with a small shape or template known as a structuring element [15][17]. In this method a morphological closing operation is performed on the red channel. The erosion operation first removes the blood vessels and then the dilation approximately restores the boundaries to their former position. The closing operation is given in equation (1).

$$\text{Closing: } I_S(A,B) = A \bullet B = E(D(A,-B),-B) \qquad (1),$$

where A is the red channel of the input image and B is a 10x10 symmetrical disc structuring element to remove the blood vessels, and IS represents the resultant vessel free, smoothed output image. Figure 1(a), Figure 1(b) and Figure 1(c) show the input image, the red channel of the input image, and the smoothed image. In the case of bright images intensity adjustment is also done.

Fig. 1. The preprocessing steps (a) Input Image (b) Red channel (c) Blood vessel Removal

B. OPtic Disc Boundary Extraction

1) Fuzzy C Means Clustering combined with Thresholding
The smoothed image *Is* is further processed for the extraction of the OD. The method presented here is a combination of Fuzzy algorithm, C Means clustering and Thresholding. Clustering involves the task of dividing data points into homogeneous classes or clusters so that items in the same class are as similar as possible and items in different classes are as dissimilar as possible. Most Fuzzy clustering algorithms are objective function based: They determine an optimal classification by minimizing an objective function. In objective function based clustering usually each cluster is represented by a cluster prototype. This prototype consists of a cluster center and maybe some additional information about the size and the shape of the cluster. The cluster center is an instantiation of the attributes used to describe the domain concerned. The size and shape parameters determine the extension of the cluster in different directions of the underlying domain. Depending on the data and the application, different types of similarity measures may be used to identify classes, where the similarity measure controls how the clusters are formed. In this new method intensity value is used as the similarity measure [18] [19]. Thresholding is one of the most powerful techniques for image segmentation in which the pixels are partitioned, depending on their intensity value, which would correspond to the background and the object [15]. The segmentation is then achieved by grouping all pixels having intensity greater than the threshold into one class, and all other pixels into another class.

2) Fuzzy C-Means Clustering Algorithm
Fuzzy C-Means (FCM) Clustering is a clustering technique which employs fuzzy partitioning such that a data point can belong to all groups with different membership grades between 0 and 1.

It is an iterative algorithm. The aim of FCM is to find cluster centers (centroids) that minimize a dissimilarity function. This algorithm works by assigning membership to each data point corresponding to each cluster center on the basis of difference between the cluster center and the data point. The more the data is near to the cluster center, the more is its membership towards the particular cluster center. Clearly, summation of the membership of each data point should be equal to 1. FCM is a method of clustering which allows one piece of data to belong to two or more clusters. It is based on minimization of the following objective function in equation (2).

$$J_m = \sum_{i=1}^{N} \sum_{j=1}^{C} u_{ij}^m \left\| x_i - c_j \right\|^2, \quad 1 \leq m < \infty \tag{2}$$

where m is any real number greater than 1, u_{ij} is the degree of membership of x_i in the cluster j, x_i is the i_{th} of d-dimensional measured data, c_j is the d-dimension center of the cluster, and $\|*\|$ is any norm expressing the similarity between any measured data and the center. Fuzzy partitioning is carried out through an iterative optimization of the objective function shown above, with the update of membership u_{ij} and the cluster centers c_j given by:

$$u_{ij} = \frac{1}{\sum_{k=1}^{C} \left(\frac{\left\| x_i - c_j \right\|}{\left\| x_i - c_k \right\|} \right)^{\frac{2}{m-1}}} \tag{3}$$

$$c_j = \frac{\sum_{i=1}^{N} u_{ij}^m \cdot x_i}{\sum_{i=1}^{N} u_{ij}^m} \tag{4}$$

This iteration will stop when

$$\max_{ij} \left\{ \left| u_{ij}^{(k+1)} - u_{ij}^{(k)} \right| \right\} < \varepsilon$$

, where ε is a termination criterion between 0 and 1, whereas k –s are the iteration steps. This procedure converges to a local minimum or a saddle point of Jm.

The algorithm is composed of the following steps:

Step 1. Initialize U= [u_{ij}] matrix, as U (0)

Step 2. At k-step: calculate the centers vectors

C $_{(k)}$ = [C_j] with U $_{(k)}$

$$u_{ij} = \frac{1}{\sum_{k=1}^{C} \left(\frac{\left\| x_i - c_j \right\|}{\left\| x_i - c_k \right\|} \right)^{\frac{2}{m-1}}} \frac{\sum_{i=1}^{N} u_{ij}^m \cdot x_i}{\sum_{i=1}^{N} u_{ij}^m}$$

Step 3. Update U (k), U (k+1)

Step4. If ∥ U (k+1) - U (k)∥< ε then STOP; otherwise return to step2. [19][20]

The Fuzzy Logic Toolbox command line function, *fcm* is used for generating clusters in this paper. This function starts with an initial guess for the cluster centers, which are intended to mark the mean location of each cluster. Next, *fcm* assigns every data point a membership grade for each cluster. In this paper three clusters are generated with low, medium and high membership grades. The outputs obtained are three cluster centers C1, C2 and C3 and membership function matrix M with membership-grades, which are the intensity values of pixels.

3) Thresholding

Thresholding is the operation of converting a multilevel image into a binary image i.e., it assigns the value of 0 (background) or 1 (objects or foreground) to each pixel of an image based on a comparison with some threshold value T (intensity or color value) [15]. As mentioned earlier the main feature of the OD is that it is having the highest intensity. The disc is extracted using the highest intensity and it is used as the threshold for the OD extraction. The threshold T is computed using the following method. From the generated clusters, first the cluster with maximum membership grade is found, and the corresponding grades are assigned with the same identification label. From the smoothed image, pixels with this gray level value are accessed, the average of the maximum and minimum intensity values are computed to obtain the threshold value T.

i.e., $\quad T = \frac{1}{2}[\text{Max (data (value))} + \text{Min (data (value))}] \tag{5}$

In the above equation, data represents the data points of the smoothed image and label represents the cluster value with the highest membership grade. By applying the threshold T on the smoothed image I_S the image is converted to a binary image I_B. The following formula (6) [15] is used for the binary image extraction.

$$I_B(x, y) = \begin{cases} 1, \text{ if } I_S (x, y) > T \\ 0, \text{ if } I_S (x, y) <= T \end{cases} \tag{6}$$

Another feature of the OD is that it is of circular shape. So the optic disc region selection process needs to be made specific to the circular region. So the largest connected component Ri whose shape is approximately circular is selected using the compactness measure

$$C (R_i) = \frac{P(Ri)}{4\pi A(\text{Ri})} \tag{7},$$

where, *P(Ri)* is the perimeter of the region Ri and *A(Ri)* is the area of the region Ri. The binary image with the compactness smaller than the pre- specified value, (5 in the present study) is considered as the optic disc approximation. Thus using the condition C < 5, extraction of round objects is done, eliminating those objects that do not meet the criteria. In some cases the extracted image contains small unwanted objects. From the extracted optic discs, it is found that the area of optic disc is greater than 2500 pixels.

Hence, in order to remove the unwanted objects, the connected components or objects that have fewer than 2500

pixels are removed from the image producing the final binary image with the OD.

Fig. 2(a) shows the extracted binary image and fig. 2(b) shows the optic disc after removal of unwanted objects.

(a)   (b)

Fig. 2.   (a) Extracted binary image (b) Extracted optic disc after   removing small objects

From the extracted OD the exterior boundary is traced using the *bwboundaries* function from the tool box and this boundary is overlaid over the ground truth image. Figure 3(a), 3(b) and 3(c) manifest the ground truth boundaries obtained from two experts, shown in green and blue, together with the optic disc boundary obtained using the new method, in white colour overlaid on the ground truth image. It can be observed that the boundary traced by the ophthalmologists and the boundary estimated by the present method are close to each other.
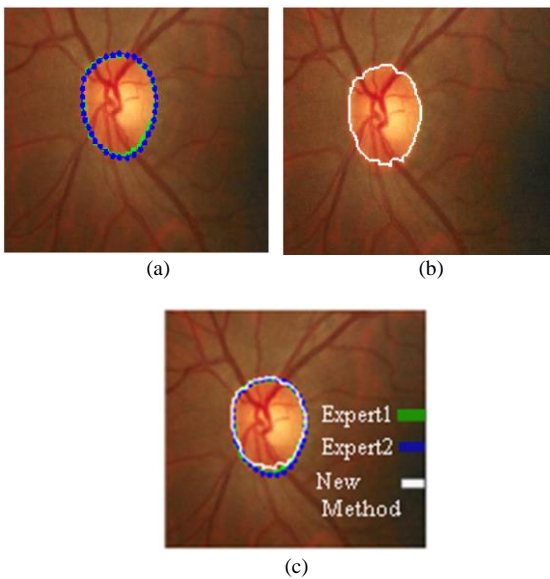

(a)   (b)

(c)

Fig. 3.   (a) Ground truth boundaries (b) extracted boundary using the new algorithm (c) Overlay of (a) and (b)

IV.   RESULTS AND DISCUSSIONS

A. Retinal Image Database

All the images used in this paper are obtained from the public database DRION-DB. It has 110 retinal images with each image having the resolution of 600 x 400 x 3 pixels and the optic disc annotated by two experts with 36 landmarks. The mean age of the patients was 53.0 years (standard Deviation 13.05), with 46.2% male and 53.8% female and all of them were Caucasian ethnicity. 23.1% patients had chronic simple glaucoma and

76.9% eye hypertension. The images were acquired with a colour analogical fundus camera, approximately centered on the ONH and they were stored in slide format. In order to have the images in digital format, they were digitized using a HP-PhotoSmart-S20 high-resolution scanner, RGB format, resolution 600 x 400 and 8 bits/pixel. Independent contours from 2 medical experts were collected by using a software tool provided for image annotation. In each image, each expert traced the contour by selecting the most significant papillary contour points and the annotation tool connected automatically adjacent points by a curve.

B. Implementation

The algorithm was applied on 110 images obtained from the DRION database. Ground truth is the OD boundary traced by 2 ophthalmologists. Five of the input image, along with their ground truth boundary as well as the detected boundary overlaid on the input image, is shown in fig.4 (a) and fig.4 (b) respectively.
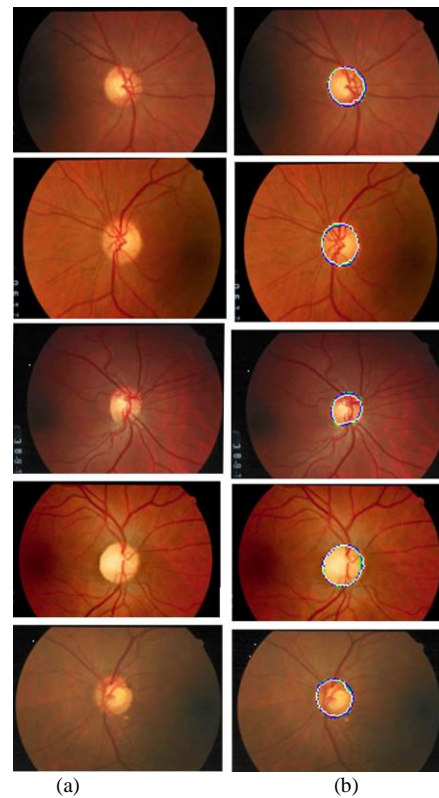

(a)   (b)

Fig. 4.   Examples for optic disc segmentation using the new algorithm (a) input image   (b) ground truth and detected boundary overlaid

C. Performance Analysis

The performance analysis is done using the following parameters.

1) Mean Difference of Diameters(MDD)

The difference between both the vertical and horizontal diameter of the detected boundary and the corresponding diameter of the actual optic disc boundary are computed. Here the actual vertical and horizontal diameters are the ground truth boundary traced by the two experts. The three vertical diameters VD1, VD2 and VD3 and the three horizontal diameters HD1,

HD2 and HD3 are calculated using the boundaries from expert 1, expert 2 and the contour obtained using the new method, using of the equations (8) and (9).

$$VD_i = Ymax_i - Ymin_i \qquad (8)$$
$$HD_i = Xmax_i - Xmin_i \quad , \qquad (9)$$

where i = 1, 2, 3 and, $Xmax_i$, $Xmin_i$, $Ymax_i$, and $Ymin_i$ are respectively the maximum and minimum coordinates of horizontal and vertical axes of the boundaries detected by expert 1, expert 2 and the present method.

Figure [5] shows the values of VD1, VD2 and VD3 as 2.9154, 2.9331 and 2.9369 and, HD1, HD2 and HD3 as 2.7671, 2.8796 and 2.9104 respectively, for a particular image. It can be seen that the 3 values of vertical diameters and 3 values of horizontal diameters are approximately the same.

Since, there was an inter-observer variability among the two experts tracing the contour of OD, therefore, the average of the contours traced by the two experts is used here. This work used as the gold standard, for each image, the average of the diameters obtained from the contours traced by the two experts

$$\text{i.e.} \quad GV = \frac{1}{2}(VD1 + VD2) \qquad (10)$$
$$GH = \frac{1}{2}(HD1 + HD2) \quad , \qquad (11)$$

where GV and GH are the gold standards of vertical and horizontal ground truth diameters respectively. That is the average of the diameters obtained from the contours traced by the two experts.

The accuracy of the detected boundary is evaluated by the parameter MDD which is the mean of the differences of the gold standard diameters calculated using the equation (12).

$$MDD = \frac{1}{2}[\frac{1}{N}\sum_{i=1}^{N}(VD_i - GV) + \frac{1}{N}\sum_{i=1}^{N}(HD_i - GH)] \qquad (12)$$

Fig. 5 shows the vertical diameter and horizontal diameter of an image with respect to expert 1, expert 2 and the new method.

As can be seen from the figure, the values of Table 1 shows the values of vertical and horizontal diameters of some of the images selected from the 110 fundus images used for the evaluation. It can be noted that the difference between the gold standard value and the value obtained by using the present method varies from 0 to 0.1298 in the case of vertical diameter and from 0 to 0.1190 in the case of horizontal diameter. The mean difference of the diameters (MDD) is evaluated as 0.0566. The smaller the MDD, the closer is the detected boundary to the ground truth.
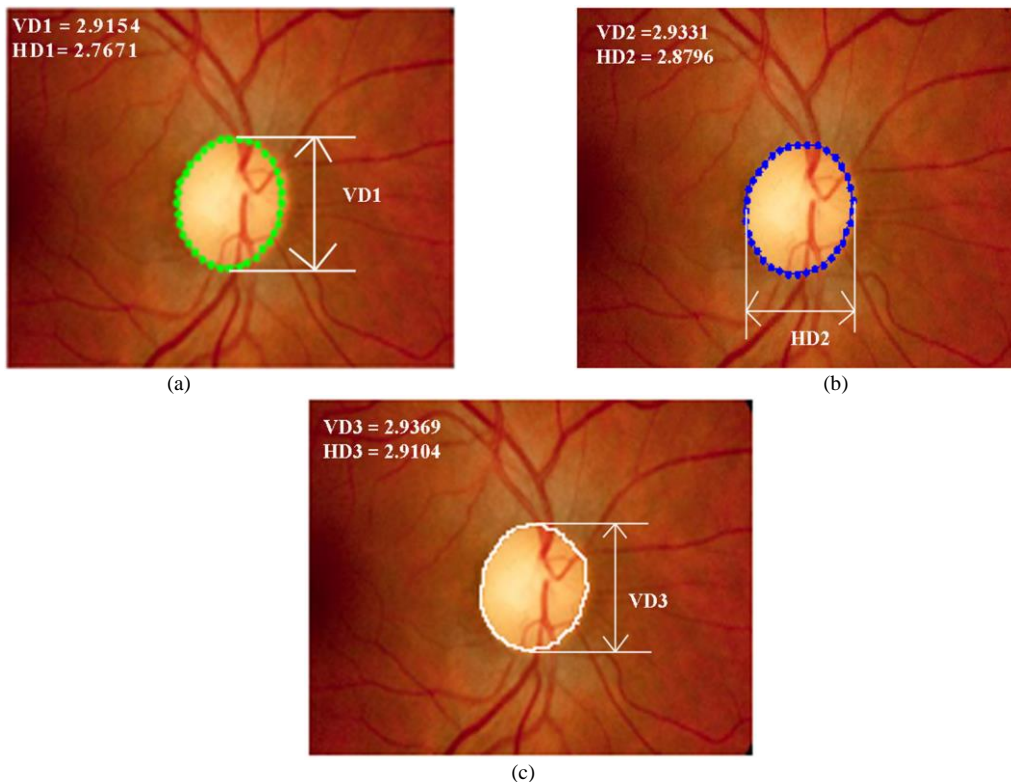

(a)

(b)

(c)

Fig. 5. The diameters obtained using the boundaries from (a) expert 1(VD1) (b) expert 2(HD2) and (c) present method (VD3)

TABLE I.   EVALUATION OF HORIZONTAL AND VERTICAL DIAMETER OF A FEW FUNDUS IMAGES

Image No.	Horizontal Diameter					Vertical Diameter				
	Expert 1 HD1	Expert 2 HD2	Gold standard GHD (1)	New Method HD3 (2)	Difference (1) - (2)	Expert 1 VD1	Expert 2 VD2	Gold standard GVD (3)	New Method VD3 (4)	Difference (3) −(4)
Img1	2.6117	2.6413	2.6265	2.6194	0.0071	2.9026	2.9962	2.9494	2.9310	0.0184
Img2	2.3266	2.2269	2.2768	2.3548	0.0780	3.2015	3.2544	3.2280	3.2015	0.0265
Img3	2.3283	2.3548	2.3416	2.3813	0.0397	2.4077	2.4606	2.4341	2.5135	0.0794
Img4	2.6988	2.6988	2.6988	2.7840	0.0852	2.8575	2.8575	2.8575	2.9698	0.1123
Img5	2.5135	2.6194	2.5665	2.6194	0.0529	2.8310	2.8310	2.8310	2.7988	0.0322
Img6	2.4181	2.4671	2.4426	2.3283	0.1143	2.3330	2.3575	2.3452	2.3019	0.0433
Img7	2.6148	2.4575	2.5362	2.6488	0.1126	2.7052	2.7374	2.7213	2.7781	0.0568
Img8	2.2906	2.1952	2.2429	2.3019	0.0590	2.3456	2.2755	2.3106	2.1960	0.1146
Img9	3.0692	3.0956	3.0824	3.0692	0.0132	3.2015	3.2544	3.2280	3.2015	0.0265
Img10	2.2225	2.2225	2.2225	2.1167	0.1058	2.0902	2.0638	2.0770	2.0902	0.0132
Img11	2.4342	2.4342	2.4342	2.4342	0	2.3548	2.3548	2.3548	2.3813	0.0265
Img12	1.9844	2.0902	2.0373	2.0646	0.0273	1.9050	1.9315	1.9183	1.9696	0.0513
Img13	2.8575	2.8575	2.8575	2.9104	0.0529	2.7781	2.8046	2.7914	2.8369	0.0455
Img14	2.7586	2.6087	2.6837	2.7517	0.0680	2.4077	2.4871	2.4474	2.5723	0.1249
Img15	2.2907	2.2788	2.2848	2.2167	0.0681	1.9653	2.1624	2.0639	2.1225	0.0586
Img16	2.6988	2.7517	2.7253	2.8104	0.0851	2.5929	2.6194	2.6062	2.6867	0.0805
Img17	2.6269	2.7008	2.6639	2.6723	0.0084	2.6723	2.6723	2.6723	2.7781	0.1058
Img18	2.5400	2.5665	2.5533	2.5665	0.0132	2.6458	2.6458	2.6458	2.6723	0.0265
Img19	2.4606	2.4606	2.4606	2.4606	0	2.7252	2.6988	2.7120	2.7517	0.0397
Img20	3.1032	3.0153	3.0593	3.0245	0.0348	3.1426	3.2215	3.1821	3.1864	0.0044
Img21	2.6194	2.6458	2.6326	2.6723	0.0397	2.7781	2.5929	2.6855	2.5871	0.0984
Img22	2.4077	2.4077	2.4077	2.4606	0.0529	2.4077	2.1960	2.3018	2.3019	0
Img23	2.6964	2.7487	2.7225	2.8046	0.0821	2.7760	2.8910	2.8335	2.9633	0.1298
Img24	2.3283	2.2857	2.3070	2.2648	0.0422	2.6683	2.5585	2.6134	2.4871	0.1263
Img25	2.5929	2.6194	2.6062	2.7252	0.1190	2.2490	2.3019	2.2754	2.3019	0.0264
Mean difference of horizontal diameter				0 .0545	Mean difference of vertical diameter				0.0587	
Mean difference of diameters(MDD)					0.0566					

2) Karl Pearson Correlation

Karl Pearson Correlation   gives the multiple correlations between the detected diameters and the ground truth diameters. Pearson Correlation is used to check the correlation between the obtained and detected diameters using the following formula.

$$r = \frac{N \sum xy - (\sum x)(\sum y)}{\sqrt{[N \sum x^2 - (\sum x)^2)][N \sum y^2 - (\sum y)^2]}} \qquad (13)$$
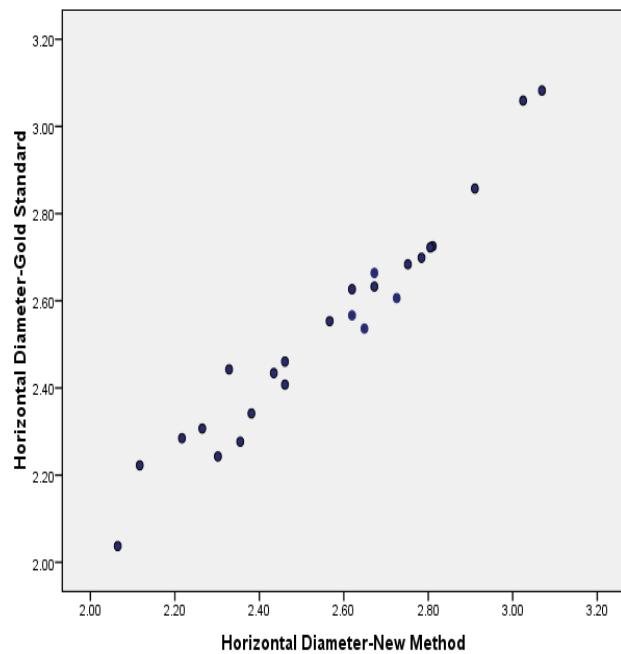
Where:

N   = number of pairs of scores
$\sum xy$ = sum of the products of the paired scores
$\sum x$ = sum of x scores
$\sum y$ = sum of y scores
$\sum x^2$ = sum of squared x scores
$\sum y^2$ = sum of squared x scores

From the 25 test images, the Pearson Correlation of the obtained horizontal and vertical diameters to the ground truth diameters with respect to the two experts are obtained as 0.946 and 0.958 and,0.94 and 0 .974 respectively.
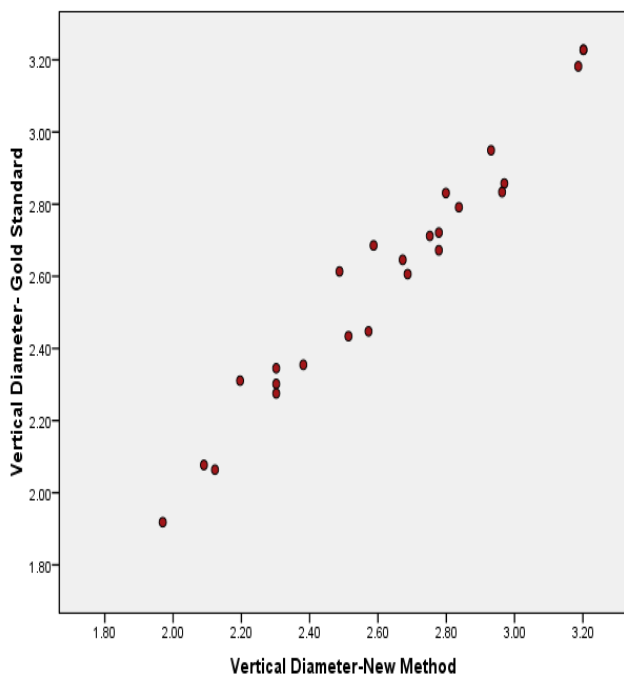
3) Scatter Plot Analysis

The scatter plot in Fig. 6(a) and Fig. 6(b) represents the detected vertical diameters Vs. the gold standard vertical diameters and detected horizontal diameters Vs. gold standard horizontal diameters with respect to the 25 test images.

It is clear from the scatter plot that there is a high positive linear correlation between the detected and the ground truth diameters.

test images, it is found that the Karl Pearson Correlation of the ground truth horizontal and vertical diameters from two experts with respect to the detected diameters are .946 & .958and .94 & .974 respectively. The scatter plot depicts a high positive correlation between the gold standard and evaluated boundaries. The present method can achieve accurate segmentation for both normal and abnormal images. The main advantage of the development of this method is that it is fully automated and can be effectively used for the extraction of optic disc boundary of retinal images, and thus to save time for retinal image screening. At the same time, it is to be observed that, it does not extract optic discs accurately in certain bright images. However, as a future enhancement the advanced clustering technique could be applied to achieve more efficient accuracy in the result in the process of optic disc extraction.

(a)

(b)

Fig. 6. Scatter plot (a) detected vs. gold standard vertical diameter (b) detected vs. gold standard horizontal diameter.

V. CONCLUSION

A reliable and practical algorithm for the extraction of optic disc is developed in this paper. Fuzzy C Means algorithm combined with thresholding is used to extract the optic disc. The performance is evaluated using the proximity of the obtained disc contour with the ground truth contours from two experts. It is found that Fuzzy C means combined with thresholding provides a result which is close to the ground truth boundary. From the 25

REFERENCES

[1] L. Gagnon, M. Lalonde, M. Beaulieu, M.-C. Boucher L. Gagnon, M. Lalonde, M. Beaulieu, M.-C. Boucher,"Procedure to detect anatomical structures in optical fundus images Procedure to detect anatomical structures in optical fundus images", Computer Research Institute of Montreal; bDept. Of Ophthalmology, Maisonneuve-Rosemont Hospital.

[2] A. D. Fleming, K. A. Goatman, S. Philip et al. "Automatic detection of retinal anatomy to assist diabetic retinopathy screening", Physics in Medicine and Biology 52, pp. 331–345, 2007.

[3] Huiqi Li, OpasChutatape, "Automatic Location of Optic Disc in retinal Images", 0-7803-6725-1/01, IEEE, pp.837 – 840, 2001

[4] Thitiporn Chanwimaluang and Guoliang Fan, "An efficient algorithm for extraction of anatomical structures in retinal images", Proc. of International Conference on Image Processing, Vol. 1, pp. 1093–1096,2003

[5] Hoover, A., Goldbaum, M., 'Locating the optic nerve in a retinal image using the fuzzy convergence of bloodvessels', IEEE Transactionson MedicalImaging, Vol.22Issue:8 pp.951 - 958 Aug. 2003

[6] Chrastek R., Wolf M., Donath K., Niemann H., Paulus D., Hothorn T., Lausen B., Lammer R., Mardin C.Y., Michelson G. 'Automated Segmentation of the Optic Nerve Head for Diagnosis of Glaucoma', Medical Image Analysis, Vol.9,pp. 297-314, 2005.

[7] Juan Xu, "Automated Optic Disc Boundary Detection by Modified Active Contour Model', IEEE Transactions on Biomedical Engineering", Vol.54, No.3, pp.473-482.2007

[8] Enrique J. Carmona, Mariano Rinco´n , Julia´n Garcı´a- , Jose´ M. Martı´nez-de-la-Casa ,"Identification of the optic nerve head with genetic algorithms", Artificial Intelligence in Medicine (2008) 43, 243—259, Elsevier 2008

[9] Echegaray,S; Soliz,P; Luo,W ,"Automatic initialization of level set segmentation for application to optic disc margin identification", CBMS 2009. 22nd IEEE International Symposium on Computer-Based Medical System, Proc. pp. 1 – 4, 2009.

[10] Welfer D, Scharcanski J, Kitamura CM, Pizzol MMD, Ludwig LWB, Marinho DR, " Segmentation of the Optic Disk in Color Eye Fundus Images Using an Adaptive Morphological Approach", Computers in Biology and Medicine, 40(2): 124-137, 2010.

[11] P. C. Siddalingaswamy and P. K. Gopalakrishna, "Automatic Localization and Boundary Detection of Optic Disc Using Implicit Active Contours", International Journal of Computer Applications, vol. 1, no. 6, pp. 1-5, 2010.

[12] Yuji Hatanaka, Atsushi Noudo, Chisako Muramatsu, Akira Sawada,Takeshi Hara, Tetsuya Yamamoto, and Hiroshi Fujita , "Automatic Measurement of Cup to Disc Ratio Based on Line Profile Analysis in Retinal Images", 33rd Annual International Conference of the IEEE EMBS Boston, Massachusetts USA, pp.3387 – 3390,August 30 - September 3,2011

[13] Amin Dehghani, Hamid Abrishami Moghaddam and Mohammad-Shahram Moin, "Optic disc localization in retinal images using histogram matching", EURASIP Journal on Image and Video Processing 2012, 2012:19 doi:10.1186/1687-5281-2012-19, 2012.

[14] Angel Suero, Diego Marin, Manuel E. Gegundez-Arias, and Jose M.

Bravo,"Locating the Optic Disc in Retinal Images Using Morphological Techniques", IWBBIO 2013. Proceedings, Granada, 18-20 March, 2013, pp.593-600, 2013.

[15] Rafael C Gonzalez, Richard E Woods, Steven L Eddins, Digital Image Processing, Prentice Hall Publications,2008.

[16] T. Walter and J. C. Klein, "Automatic analysis of colour fundus photographs and its application to the diagnosis of diabetic retinopathy," in Handbook of Biomedical Image Analysis. New York: Kluwer, vol. 2, pp. 315–368 2005.

[17] Rafael C Gonzalez, Richard E Woods, Steven L Eddins., Digital Image Processing Using Matlab, Prentice Hall Publications, 2004.

[18] Yinghua Lu, Tinghuai Ma, Changhong Yin, Xiaoyu Xie, Wei Tian,ShuiMing Zhong, " Implementation of the Fuzzy C-Means Clustering Algorithm in Meteorological Data", International Journal of Database Theory and Application, Vol.6, No.6, pp.1-18, 2013.

[19] HeikoTimm, Christian Borgelt, and Rudolf KruseFuzzy, " Cluster Analysis with Cluster Repulsion",CiteSeerx.

[20] Yong Yang , Shuying Huang, " Image segmentation by fuzzy c-means Clustering algorithm with a novel Penalty term", Computing and Informatics, Vol. 26, pp. 17–31, 2007.